Optical properties of monolayer transition metal dichalcogenides probed by spectroscopic ellipsometry

Hsiang-Lin Liu, Chih-Chiang Shen, Sheng-Han Su, Chang-Lung Hsu, Ming-Yang Li, and Lain-Jong Li

Citation: Applied Physics Letters **105**, 201905 (2014); doi: 10.1063/1.4901836
View online: http://dx.doi.org/10.1063/1.4901836
View Table of Contents: http://scitation.aip.org/content/aip/journal/apl/105/20?ver=pdfcov
Published by the AIP Publishing

Optical properties of monolayer transition metal dichalcogenides probed by spectroscopic ellipsometry

Hsiang-Lin Liu,[1,a)] Chih-Chiang Shen,[1] Sheng-Han Su,[2] Chang-Lung Hsu,[2] Ming-Yang Li,[2] and Lain-Jong Li[2,b)]
[1]*Department of Physics, National Taiwan Normal University, Taipei 11677, Taiwan*
[2]*Institute of Atomic and Molecular Sciences, Academia Sinica, Taipei 10617, Taiwan*

(Received 21 August 2014; accepted 3 November 2014; published online 18 November 2014)

Spectroscopic ellipsometry was used to characterize the complex refractive index of chemical-vapor-deposited monolayer transition metal dichalcogenides (TMDs). The extraordinary large value of the refractive index in the visible frequency range is obtained. The absorption response shows a strong correlation between the magnitude of the exciton binding energy and band gap energy. Together with the observed giant spin-orbit splitting, these findings advance the fundamental understanding of their novel electronic structures and the development of monolayer TMDs-based optoelectronic and spintronic devices. © *2014 AIP Publishing LLC*. [http://dx.doi.org/10.1063/1.4901836]

The layered transition metal dichalcogenides (TMDs), including MX_2 (M = Mo, W; X = S, Se, Te), have recently attracted considerable attention due to their novel physical phenomena in reduced dimension and the spatially confined electronic and optical properties.[1,2] Among them, monolayer TMDs are special in many respects. Most notably, monolayer TMDs have a rather large direct bandgap, making these materials favourable for optoelectronic applications,[3–8] field-effect transistors,[9–11] and photovoltaic cells.[12] Furthermore, both the conduction and valence bands of monolayer TMDs have two energy degenerate valleys at the corners of the first Brillouin zone, which are essential to optically control the charge carriers in these valleys.[13] These properties make possible a new class of integration in spintronics and valleytronics.[14–16]

For many of these applications, knowledge of the optical properties of monolayer TMDs is fundamentally important. From photoluminescence characterization, information about the optical bandgap of these materials can be gained.[3–8] The observed double-peak structure in the optical absorption spectra of monolayer TMDs can be connected to exciton excitations. These excitons are due to the vertical transition at the *K* point of the Brillouin zone from a spin-orbit-split valence band to doubly degenerate conduction band.[17] Despite the intense research on the optical properties of monolayer TMDs, no studies of their wavelength-dependent complex refractive index have been done to date. Measurements of the refractive index and extinction coefficient spectra of monolayer TMDs over a wide frequency range can provide useful information about optical and electronic properties that devices based on these materials may possess.

In this paper, we combine a spectroscopic ellipsometry with a series of monolayer TMDs materials to more deeply explore their optical constants ranging from the near-infrared to the deep-ultraviolet. Spectroscopic ellipsometry allows the determination of a material's optical functions, such as refractive index and extinction coefficient, and thickness of thin films in a nondestructive manner.[18] We find that monolayer MoS_2 displays extraordinary large value of the refractive index about 6.50 at 450 nm. It decreases to 4.25 at 540 nm for monolayer $MoSe_2$. Moreover, the absorption edge in extinction coefficient spectra reveals that monolayer WS_2 has the largest band gap of about 2.11 eV. It decreases to 1.62 eV for monolayer $MoSe_2$. Notably, a direct correlation is observed between the magnitude of bang gap and exciton binding energy in monolayer TMDs. Additionally, the spin-orbit splitting energy of monolayer TMDs increases as the fourth power of the atomic number of the constituent elements. This work advances the development of monolayer TMDs materials with coexisting optoelectronic and spintronics device components.

Monolayer TMDs thin films, such as MoS_2, $MoSe_2$, WS_2, and WSe_2, were deposited onto sapphire substrates by chemical vapor deposition.[19–22] These thin films were high-quality single layer materials verified using atomic force microscopy.[19–22] Micro-Raman scattering spectroscopy was also performed to characterize the thickness and structural quality of the thin films. The experimental results of several points across the thin films indicate one layer signature.[19–23]

Ellipsometric spectra were collected under multiple angles of incidence between 60° and 75° using a Woollam M-2000U rotating compensator multichannel spectroscopic ellipsometer over a spectral range from 0.73 to 6.42 eV. The reproducibility of the spectra were also confirmed at three different spots on the thin films using a specially designed focusing optics coupled with spectroscopic ellipsometry for the spot ($100 \times 100\ \mu m^2$) measurements. The complex dielectric functions of monolayer TMDs thin films were extracted using least-squares regression analysis and weighted root-mean-square error to fit the ellipsometric spectra to a stacked layer model consisting of sapphire substrate/thin film/surface roughness/air ambient structure. The parameters of the stacked layer model used to fit the raw ellipsometry data are listed in Table I.

Figure 1 shows the refractive index and extinction coefficient spectra of monolayer MoS_2, $MoSe_2$, WS_2, and WSe_2 thin films in the wavelength range from 193 to 1700 nm. In all cases, the refractive indices increase with increasing

a)Author to whom correspondence should be addressed. Electronic mail: hliu@ntnu.edu.tw
b)Present address: Physical Science and Engineering Division, King Abdullah University of Science and Technology, Thuwal 23955-6900, Kingdom of Saudi Arabia.

TABLE I. Parameters of a stacked layer model fit for monolayer TMDs. All units are in nm.

	MoS_2	$MoSe_2$	WS_2	WSe_2
Sapphire substrate	1 (mm)	1 (mm)	1 (mm)	1 (mm)
Film	0.71	0.97	0.81	0.76
Roughness	0.11	0.17	0.13	0.19

wavelength in the spectral range from 193 nm to 550 nm, and then approach the maxima, and decrease with the wavelength until 1700 nm. Two items merit special attention. First, the dispersive response in the refractive index exhibits several anomalous dispersion features below 800 nm and approaches a constant value of 3.5–4.0 in the near-infrared frequency range. Second, monolayer MoS_2 has the extraordinary large value of the refractive index about 6.50 at 450 nm. The maxima of refractive index around 6.25 at 445 nm, 5.68 at 540 nm, and 4.25 at 540 nm are observed for monolayer WS_2, WSe_2, and $MoSe_2$, respectively. The characteristics of high refractive index observed in the visible frequency range for these monolayer TMDs thin films have many potential applications, such as good antireflection coatings for photonics and optoelectronics,[24] high performance substrates for advanced display devices,[25] and optical encapsulants for the enhancement of photovoltaic cell response.[26] In Fig. 1, the extinction coefficient spectra show several strong absorptions below 700 nm. These dispersion peaks are due to the optical transitions, with detailed analysis shown below.

Figure 2 displays the absorption spectra of monolayer MoS_2, $MoSe_2$, WS_2, and WSe_2 thin films. The absorption spectra can be divided into a region at low energy, which are dominated by excitonic transitions on a relatively low absorption background and a region of strong absorption at higher energies. The discrete states of the exciton observed in monolayer TMDs thin film can be modeled by using a broadened Lorentzian line shape[27]

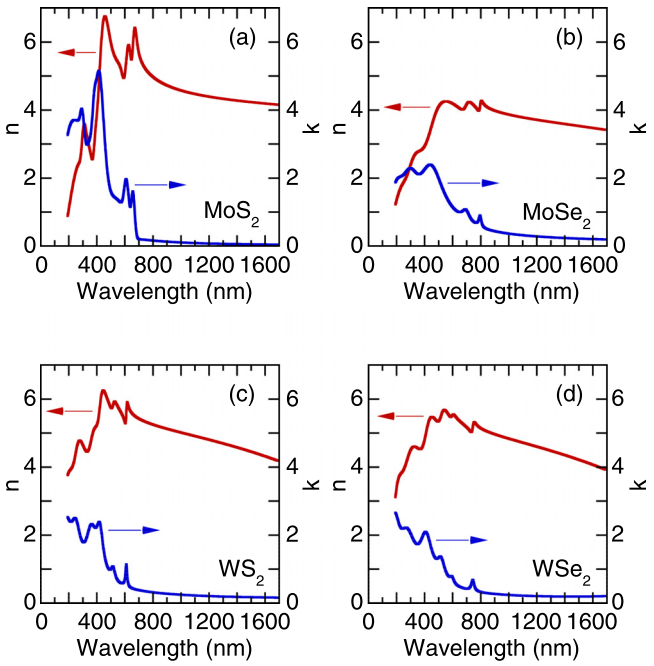

FIG. 1. Refractive index n and extinction coefficient k of monolayer (a) MoS_2, (b) $MoSe_2$, (c) WS_2, and (d) WSe_2 thin films.

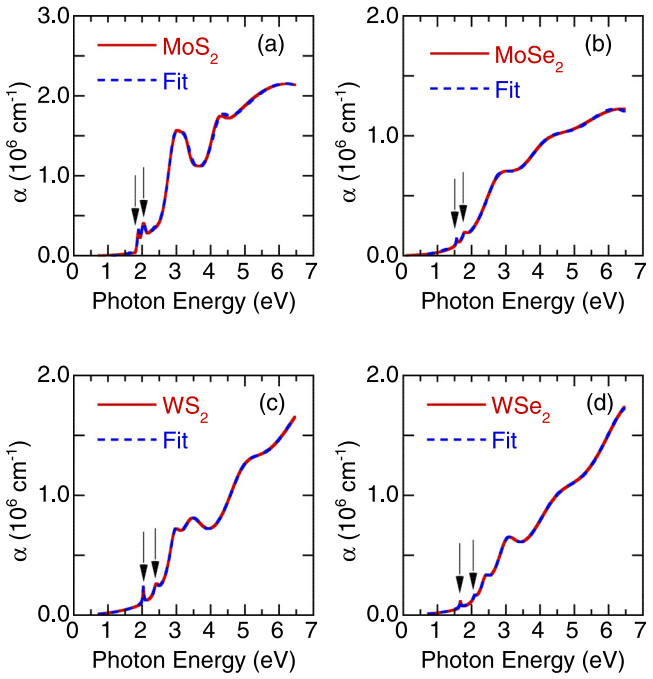

FIG. 2. Optical absorption coefficient α of monolayer (a) MoS_2, (b) $MoSe_2$, (c) WS_2, and (d) WSe_2 thin films. The dashed line is the best fit using a broadened Lorentzian line shape. The arrow denotes the exciton peaks.

$$\alpha(E) = \mathrm{Im}\left[\sum_{n=A,B}\left(\sum_{m=1}^{\infty}\frac{A_{0n}^{ex}}{m^3}\frac{1}{E_{0n}-\frac{R_n}{m^2}-E-i\Gamma_{ex,m}}\right)\right], \quad (1)$$

where n is the index number of the valence band, m is the index number of the excited state of the exciton, R_n is the exciton Rydberg constant, $\Gamma_{ex,m}$ is a broadening parameter of the mth excited exciton state, E_{0n} is the band gap energy, and A_{0n}^{ex} is an adjustable fitting parameter. For common two-dimensional materials, the ground-state exciton binding energy is given by $E_b^{2D} = 4R_n$.[28] Our fitting curves are shown in Fig. 2. A list of fitting parameters is given in Table II. Monolayer WS_2 has the largest band gap of about 2.11 eV. It decreases to 1.95, 1.72, and 1.62 eV for monolayer MoS_2, WSe_2, and $MoSe_2$, respectively. Our results are close to the values reported by photoluminescence experiments in mechanically exfoliated monolayer MoS_2,[3–5] $MoSe_2$,[5] WS_2,[6,7] and WSe_2,[7] and angle-resolved photoemission spectroscopic (ARPES) studies in molecular beam epitaxy grown monolayer $MoSe_2$.[29]

As indicated in Fig. 2, we found very clear excitonic absorption peaks A and B for all monolayer TMDs. They originate from the spin-split direct gap transitions at the K point of the Brillouin zone. According to Table II, the values of A-exciton binding energy are estimated to be about 0.32, 0.28, 0.24, and 0.24 eV for monolayer WS_2, MoS_2, WSe_2, and $MoSe_2$, respectively. The result of monolayer MoS_2 is in reasonable agreement with recent scanning tunneling microscopy and spectroscopy and photoluminescence experiments estimate of 0.22 ± 0.1 eV.[30] However, all of the experimental data are lower than the current first-principles calculations by about 0.4–0.7 eV.[31–35] This difference might come from the 0 K first-principles frameworks. The exciton binding energy increases when the temperature is lowered. Another

TABLE II. The exciton band gap energies, exciton binding energies, and exciton broadening parameters of monolayer TMDs.

	MoS_2	$MoSe_2$	WS_2	WSe_2
A-exciton energy gap (eV)	1.95 ± 0.01	1.62 ± 0.01	2.11 ± 0.01	1.72 ± 0.01
A-exciton binding energy (eV)	0.28 ± 0.005	0.24 ± 0.005	0.32 ± 0.005	0.24 ± 0.005
A-exciton (eV) $\Gamma_{ex,1}$ (eV)	0.05 ± 0.005	0.01 ± 0.005	0.02 ± 0.005	0.02 ± 0.005
B-exciton energy gap (eV)	2.08 ± 0.01	1.82 ± 0.01	2.45 ± 0.01	2.09 ± 0.01
B-exciton binding energy (eV)	0.16 ± 0.005	0.08 ± 0.005	0.12 ± 0.005	0.08 ± 0.005
B-exciton (eV) $\Gamma_{ex,1}$ (eV)	0.09 ± 0.005	0.07 ± 0.005	0.06 ± 0.005	0.03 ± 0.005

interesting observation in Fig. 2 is that we found a good correlation between the exciton binding energy and band gap energy in monolayer TMDs. A plot of this correlation is shown in Fig. 3(a). We see a simple relation ($E_b^{2D} = 0.18\,\text{eV} + 6.4 \times 10^{-3}\, E_g^{\,4}$) that holds for all monolayer TMDs. This general expression can be interpreted in a number of different ways. One of the most possible explanations is that the exciton binding energy is given by $E_b = \mu_{ex} e^4 / 2\hbar^2 \varepsilon_0^2$, where $\mu_{ex} = m_e m_h/(m_e + m_h)$ is the effective exciton mass and ε_0 is the static dielectric constant.[28] Penn has proposed a simple two-band model with an average band gap E_g (known as the Penn gap) to account for ε_0 in a semiconductor.[36] In this theory, ε_0 is given by $\varepsilon_0 = 1 + (E_p/E_g)^2$, where E_p is the plasma energy of the valence electrons, and allowing that the exciton binding energy increases as the fourth power of the band gap energy for all monolayer TMDs, which in agreement with our measurements.

For monolayer TMDs, the valence-band spin-orbit splitting at the K point can be estimated from the energy difference between the A and B exciton peaks. Our findings of the spin-orbit coupling of ~150, 240, 380, and 420 meV in monolayer MoS_2, $MoSe_2$, WS_2, and WSe_2 are consistent with the previous theoretical predictions,[17,31–35,37] differential reflectance experiments in mechanically exfoliated monolayer WS_2 and WSe_2,[7] and ARPES studies in molecular beam epitaxy grown monolayer $MoSe_2$.[29] In Fig. 3(b), we plot the spin-orbit splitting energy Δ_{so} for different monolayer TMDs as a function of average atomic number Z_{av}. By fitting the data depicted in Fig. 3(b), a general expression can be obtained and is given by $\Delta_{so} = 115\,\text{meV} + 6.0 \times 10^{-4}\, Z_{av}^{\,4}$. The spin-orbit splitting energy of monolayer TMDs increases as the fourth power of the average atomic number of the constituent elements. The atomic $\boldsymbol{L}\cdot\boldsymbol{S}$ interaction provides a framework within which we can understand this trend.[38] Our analysis reveals that the larger value of the spin-orbit splitting in monolayer WSe_2 gives it greater application potential than other monolayer TMDs in spintronics devices.

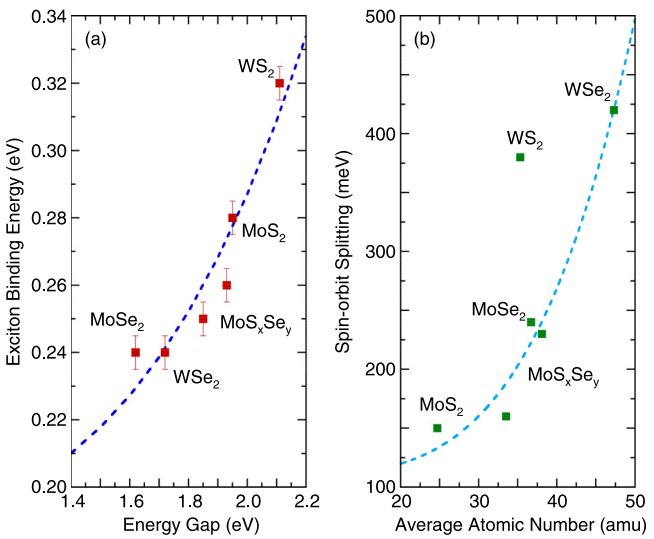

FIG. 3. (a) The exciton binding energy vs. band gap energy for different monolayer TMDs. MoS_xSe_y is monolayer alloy.[22] The dashed line is from $E_b^{2D} = 0.18\,\text{eV} + 6.4 \times 10^{-3}\, E_g^{\,4}$. (b) The spin-orbit splitting energy vs. average atomic number for different monolayer TMDs. The dashed line is from $\Delta_{so} = 115\,\text{meV} + 6.0 \times 10^{-4}\, Z_{av}^{\,4}$.

In summary, we employed the spectroscopic ellipsometry to investigate the optical properties of monolayer TMDs. The extraordinary large value of the refractive index about 6.50 in the visible frequency range is obtained for monolayer MoS_2. The absorption emerging in extinction coefficient spectra shows that monolayer WS_2 has the largest band gap of about 2.11 eV. It decreases to 1.62 eV for monolayer $MoSe_2$, a result that demonstrates band gap tunability in these systems. Furthermore, a direct correlation is observed between the magnitude of the exciton binding energy E_b^{2D} and band gap energy E_g in monolayer TMDs, E_b^{2D} is proportional to $E_g^{\,4}$. The spin-orbit splitting energy also increases as the fourth power of the average atomic number of the constituent elements, leading to the giant spin-orbit splitting (~420 meV) in monolayer WSe_2. These findings not only extend our understandings of novel electronic structures of monolayer TMDs but also provide the foundation for future technological applications of optoelectronic and spintronic device components.

We thank M. C. Chang for stimulating discussions and financial support from the Ministry of Science and Technology of the Republic of China under Grant No. NSC 102-2112-M-003-002-MY3.

[1]Q. H. Wang, K. Z. Kourosh, A. Kis, J. N. Coleman, and M. S. Strano, Nat. Nanotechnol. **7**, 699 (2012).
[2]M. Chhowalla, H. S. Shin, G. Eda, L. J. Li, K. P. Loh, and H. Zhang, Nat. Chem. **5**, 263 (2013).

[3]K. F. Mak, C. Lee, J. Hone, J. Shan, and T. F. Heinz, Phys. Rev. Lett. **105**, 136805 (2010).
[4]A. Splendiani, L. Sun, Y. Zhang, T. Li, J. Kim, C. Y. Chim, G. Galli, and F. Wang, Nano Lett. **10**, 1271 (2010).
[5]S. Tongay, J. Zhou, C. Ataca, K. Lo, T. S. Matthews, J. Li, J. C. Grossman, and J. Wu, Nano Lett. **12**, 5576 (2012).
[6]H. R. Gutuerrez, N. Perea-Lopez, A. L. Elias, A. Berkdemir, B. Wang, R. L. F. López-Urias, V. H. Crespi, H. Terrones, and M. Terrones, Nano Lett. **13**, 3447 (2013).
[7]W. Zhao, Z. Ghorannevis, L. Chu, M. Toh, C. Kloc, P. H. Tan, and G. Eda, ACS Nano **7**, 791 (2013).
[8]R. S. Sundaram, M. Engel, A. Lombardo, R. Krupke, A. C. Ferrari, Ph. Avouris, and M. Steiner, Nano Lett. **13**, 1416 (2013).
[9]B. Radisavljevic, A. Radenovic, J. Brivio, V. Giacometti, and A. Kis, Nat. Nanotechnol. **6**, 147 (2011).
[10]B. Radisavljevic, M. B. Whitwick, and A. Kis, ACS Nano **5**, 9934 (2011).
[11]S. Larentis, B. Fallahazad, and E. Tutuc, Appl. Phys. Lett. **101**, 223104 (2012).
[12]M. Bernardi, M. Palummo, and J. C. Grossman, Nano Lett. **13**, 3664 (2013).
[13]D. Lagarde, L. Bouet, X. Marie, C. R. Zhu, B. L. Liu, T. Amand, P. H. Tan, and B. Urbaszek, Phys. Rev. Lett. **112**, 047401 (2014).
[14]K. F. Mak, K. He, J. Shan, and T. F. Heinz, Nat. Nanotechnol. **7**, 494 (2012).
[15]H. Zeng, J. Dai, W. Yao, D. Xiao, and X. Cui, Nat. Nanotechnol. **7**, 490 (2012).
[16]T. Cao, G. Wang, W. Han, H. Ye, C. Zhu, J. Shi, Q. Niu, P. Tan, E. Wang, B. Liu, and J. Feng, Nat. Commun. **3**, 887 (2012).
[17]Z. Y. Zhu, Y. C. Cheng, and U. Schwingenschlogl, Phys. Rev. B **84**, 153402 (2011).
[18]H. G. Tompkins and W. A. McGahan, *Spectroscopic Ellipsometry and Reflectometry: A User's Guide* (John Wiley & Sons, New York, 1999).
[19]Y. H. Lee, X. Q. Zhang, W. Zhang, M. T. Chang, C. T. Lin, K. D. Chang, Y. C. Yu, T. W. Wang, C. S. Chang, L. J. Li, and T. W. Lin, Adv. Mater. **24**, 2320 (2012).
[20]Y. H. Lee, L. Yu, H. Wang, W. Fang, X. Ling, Y. Shi, C. T. Lin, J. K. Huang, M. T. Chang, C. S. Chang, M. Dresselhaus, T. Palacios, L. J. Li, and J. Kong, Nano Lett. **13**, 1852 (2013).
[21]J. K. Huang, J. Pu, C. L. Hsu, M. H. Chiu, Z. Y. Juang, Y. H. Chang, W. H. Chang, Y. Iwasa, T. Takenobu, and L. J. Li, ACS Nano **8**, 923 (2014).
[22]S. H. Su, Y. T. Hsu, Y. H. Chang, M. H. Chiu, C. L. Hsu, W. T. Hsu, W. H. Chang, J. H. He, and L. J. Li, Small **10**, 2589 (2014).
[23]C. C. Shen, Y. T. Hsu, L. J. Li, and H. L. Liu, Appl. Phys. Express **6**, 125801 (2013).
[24]D. Bouhafs, A. Moussi, A. Chikouche, and J. M. Ruiz, Sol. Energy Mater. Sol. Cells **52**, 79 (1998).
[25]T. Nakamura, H. Fujii, N. Juni, and N. Tsutsumi, Opt. Rev. **13**, 104 (2006).
[26]M. Ma, F. W. Mont, D. J. Poxson, J. Cho, E. F. Schubert, R. E. Welser, and A. K. Sood, J. Appl. Phys. **108**, 043102 (2010).
[27]J. F. Muth, R. M. Kolbas, A. K. Sharma, S. Oktyabrsky, and J. Narayan, J. Appl. Phys. **85**, 7884 (1999).
[28]M. Shinada and S. Sugano, J. Phys. Soc. Jpn. **21**, 1936 (1966).
[29]Y. Zhang, T. R. Chang, B. Zhou, Y. T. Cui, H. Yan, Z. Liu, F. Schmitt, J. Lee, R. Moore, Y. Chen, H. Lin, H. T. Jeng, S. K. Mo, Z. Hussain, A. Bansil, and Z. X. Shen, Nat. Nanotechnol. **9**, 111 (2014).
[30]C. Zhang, A. Johnson, C. L. Hsu, L. J. Li, and C. K. Shih, Nano Lett. **14**, 2443 (2014).
[31]A. Ramasubramaniam, Phys. Rev. B **86**, 115409 (2012).
[32]T. Cheiwchanchamnangij and W. R. L. Lambrecht, Phys. Rev. B **85**, 205302 (2012).
[33]H. P. Komsa and A. V. Krasheninnikov, Phys. Rev. B **86**, 241201 (2012).
[34]H. Shi, H. Pan, Y. W. Zhang, and B. I. Yakobson, Phys. Rev. B **87**, 155304 (2013).
[35]D. Y. Qiu, F. H. da Jornada, and S. G. Louie, Phys. Rev. Lett. **111**, 216805 (2013).
[36]D. R. Penn, Phys. Rev. **128**, 2093 (1962).
[37]A. Molina-Sanchez, D. Sangalli, K. Hummer, A. Marini, and L. Wirtz, Phys. Rev. B **88**, 045412 (2013).
[38]P. Y. Yu and M. Cardona, *Fundamentals of Semiconductors: Physics and Materials Properties* (Springer, Heidelberg, 1996), pp. 67–77.